Longshore Currents and the Onset of Upwelling over Bottom Slope

J. PEDLOSKY

Dept. of the Geophysical Sciences, The University of Chicago

(Manuscript received 18 January 1974, in revised form 10 April 1974)

ABSTRACT

The evolution of longshore currents produced by upwelling on an f-plane over shelf-like bottom topography for times long compared to a barotropic spin-up time, but short compared to a diffusion time, reveals in a linear, time-dependent, three-dimensional model that:

1. The topographic constraints yield a *steady* topographic boundary layer on these short time scales similar in structure to the layer found in an earlier steady-state model.
2. Within a Rossby radius of deformation of the coast a swift equatorward longshore current with a poleward countercurrent is formed.
3. Wind-stress forcing with large north-south scales are the most efficient in driving longshore currents, but do not effectively produce internal Kelvin waves, as do the shorter longshore scales of forcing.

1. Introduction

The structure of longshore currents in coastal upwelling zones has drawn the attention of theorists and observationalists primarily because it is a relatively easily observed signature and consequence of the more difficult to observe upwelling circulation in planes perpendicular to the coast. The longshore current consists of a relatively swift surface current with velocities of the order of 20 cm sec^{-1} and an offshore scale of order 20–30 km. This surface current flows toward the equator. At depth a somewhat weaker poleward countercurrent is frequently observed. This countercurrent is relatively broad. According to Allen (1973a) it has a width of O(20–100 km) and seems to be coupled to the shelf and slope topography. A deep countercurrent is also occasionally (Huyer *et al.*, 1973) reported in the nearshore area nestled against the coast.

In a recent paper (Pedlosky, 1974; hereafter referred to as P), I considered the role of topography in a simple steady-state, three-dimensional model and showed that the vorticity constraint associated with the bottom slope could give rise to a broad poleward countercurrent if there was a net onshore transport in the region seaward of the upwelling zone.

The purpose of the present paper is to relax the condition of steadiness and study the transient onset of upwelling 1) to determine the time required to set up the barotropic, topographically associated flow, and 2) to investigate the structure of the baroclinic current on a time scale long compared with a barotropic spin-up time but short compared with the vertical diffusion time after which the results of the earlier calculation in P apply.

The major results of the present paper show (i) that (not surprisingly) the barotropic, steady-state topographic layer in P is formed in the relatively short barotropic spin-up time, (ii) the quasi-steady baroclinic flow set-up, after bottom friction has sufficient time to operate, contains a poleward countercurrent nestled against the coast (*This* inshore countercurrent will dissipate over the longer diffusion time scale and was not present in P.), and (iii) that internal Kelvin waves are not likely to be produced by the long north-south scales of forcing which are the most efficient in producing longshore currents.

The inshore countercurrent is similar to the one produced in the numerical β-plane calculation of Hurlburt and Thompson (1973), although in my own mind the present model has certain advantages. The structure of the current is found here for a continuously stratified as opposed to a two-layer model. The two-layer model has the disadvantage of blending in an indeterminate way the inviscid onshore flow (which leads to a longshore acceleration), and the bottom boundary layer onshore flow which does not. The present theory also presents an explicit and rather clearer recipe for the determination of the longshore pressure gradient. As in P, the β-effect is neglected and only the topographic slope contributes to the vorticity constraint in view of the latter's numerical dominance in the upwelling zone. The presence of β is accepted implicitly insofar as it leads here, as in P, to the condition of interrupted geostrophic contours (isopleths of f/depth). The present calculation also has the advantage of yielding the structure of the quasi-steady, baroclinic longshore flow in an easily accessible, closed-form, analytical solution.

2. The model

The model is substantially the same as in P, i.e., a channel on the f-plane of width L (see Fig. 1). The top of the channel is flat but the bottom slopes uniformly upward in the x-direction. The x-direction is identified as eastward and the y-direction northward. The region is implicitly considered closed in the sense (as discussed in P) that geostrophic contours (lines of constant f/H, where H is the depth) are interrupted at some latitude y_0 south of the region of interest. The north-south scale of the motion is taken to be large with respect to L and is determined by the scale of the applied wind stress τ^*, which is switched on at $t=0$ and then held steady. This is a crude model for the often rapid initiation or strengthening of upwelling. The characteristic amplitude of the applied wind stress is τ_0.

The fluid is assumed to be incompressible and continuously stratified with a constant static stability. The coefficients of turbulent mixing of momentum and heat (or density) in the vertical are ν_v and κ_v, respectively. The corresponding horizontal mixing coefficients ν_H and κ_H play a relatively minor role in the present study. A characteristic velocity $U=\tau_0/[\rho_0(\nu_v\Omega)^{\frac{1}{2}}]$, where ρ_0 is the mean density and Ω is one-half the Coriolis parameter, appropriate for the upper Ekman layer, is used to scale the horizontal velocity fields. The bottom slopes upward at an angle α from $x=0$ where the depth is D, to the eastern side of the channel where the depth is $d=d_0D$. I assume throughout that d is much larger than the Ekman depth $(\nu_v/\Omega)^{\frac{1}{2}}$.

The scaling relations between the starred, dimensional variables and their unstarred, nondimensional counterparts are

$$\left.\begin{aligned}(u_*,v_*,w_*)&=U\left(u,v,\frac{D}{L}w\right)\\(x_*,y_*,z_*)&=L\left(x,y,\frac{D}{L}z\right)\\t_*&=t/(2\Omega T)\\\Delta p_*&=2\rho_0U\Omega Lp\\\Delta\rho_*&=2\rho_0\frac{U\Omega L}{gd}\rho\\\tau_*&=\tau_0\tau\end{aligned}\right\},\tag{2.1}$$

where u_*, v_*, w_* are the velocities in the x, y, z directions. The functions Δp_* and $\Delta\rho_*$ are the pressure and density anomalies, while ρ_0 is the mean density of the "Boussinesq" fluid. The parameter T is a nondimensional *inverse* time characteristic of the evolution of the upwelling process, and, as shown below, of $O[(\nu_v/\Omega)^{\frac{1}{2}}D^{-1}]$, i.e., *small*.

In nondimensional units the equations for the bottom

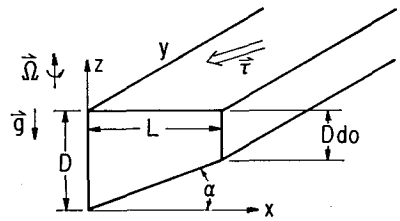

FIG. 1. The domain of the problem.

becomes

$$z_s=x\tan\theta,$$

where

$$\tan\theta=1-d_0=(L/D)\tan\alpha.$$

The model equations, as in P, are the linear versions of the momentum and heat equations completed by the condition of incompressibility, *viz*:

$$T\frac{\partial u}{\partial t}-v=-\frac{\partial p}{\partial x}+\frac{E_v}{2}\frac{\partial^2u}{\partial z^2}+\frac{E_H}{2}\left(\frac{\partial^2u}{\partial x^2}+\frac{\partial^2u}{\partial y^2}\right)\tag{2.2a}$$

$$T\frac{\partial v}{\partial t}+u=-\frac{\partial p}{\partial y}+\frac{E_v}{2}\frac{\partial^2v}{\partial z^2}+\frac{E_H}{2}\left(\frac{\partial^2v}{\partial x^2}+\frac{\partial^2v}{\partial y^2}\right)\tag{2.2b}$$

$$0=-\frac{\partial p}{\partial z}-\rho\tag{2.2c}$$

$$T\frac{\partial\rho}{\partial t}-wS=\frac{E_v}{2\sigma_v}\frac{\partial^2\rho}{\partial z^2}+\frac{E_H}{2\sigma_H}\left(\frac{\partial^2\rho}{\partial x^2}+\frac{\partial^2\rho}{\partial z^2}\right)\tag{2.2d}$$

$$\frac{\partial u}{\partial x}+\frac{\partial v}{\partial y}+\frac{\partial w}{\partial z}=0.\tag{2.2e}$$

A linear density-temperature relation is implicitly assumed in (2.2d) while (2.2c) depends on the mild requirement of hydrostatic balance. The nondimensional parameters in (2.2) are

$$\left.\begin{aligned}E_v&=\nu_v/(\Omega D^2)\\E_H&=\nu_H/(\Omega L^2)\\S&=N^2D^2/(4\Omega^2L^2)\\\sigma_v&=\nu_v/\kappa_v\\\sigma_H&=\nu_H/\kappa_H\\T&=\tfrac{1}{2}\Omega T_*\end{aligned}\right\},\tag{2.3}$$

where N is the constant Brunt frequency characterizing the stable density gradient of the basic state, and T_* is the *dimensional* time scale of the motion. Another significant parameter is $\tan\theta$ which, as in P, is taken to be larger than $E_v^{\frac{1}{2}}$ (which is realistic and important) while for technical reasons I assume it to be small with respect to 1.

The boundary conditions for the velocity are

$$\left.\begin{aligned}(u,v,w)&=E_v^{-\frac{1}{2}}[\tau^{(x)},\tau^{(y)},0],\quad\text{on}\quad z=1\\(u,v,w)&=(0,0,0),\quad\text{on}\quad z=z_s\\(u,v)&=(0,0),\quad\text{on}\quad x=0,\,1\end{aligned}\right\},\tag{2.4}$$

where $\tau^{(x)}$ and $\tau^{(y)}$ are the x and y components of τ. The density field satisfies insulating conditions on $x=0$ and z_s not relevant to the present study.

The problem is solved under the parameter restrictions

$$E_v^{\frac{1}{2}} \ll \lambda \sigma_H S \lesssim 1, \tag{2.5a}$$

$$\sigma_H = O(\sigma_v) = O(1), \tag{2.5b}$$

$$E_v^{\frac{1}{2}} \ll \tan\theta \ll 1, \tag{2.5c}$$

$$T \ll 1, \tag{2.5d}$$

$$\lambda > O(1), \tag{2.5e}$$

where $\lambda = E_v/E_H$.

As in P the most convenient approach to the problem is through boundary layer theory.

Two derived equations from (2.2) are of interest. Elimination of the pressure between (2.2a) and (2.2b) with the subsequent elimination of w with the aid of (2.2d) yields the potential vorticity equation

$$T\frac{\partial}{\partial t}\left[\zeta - S^{-1}\frac{\partial \rho}{\partial z}\right] = \frac{E_v}{2}\frac{\partial^2}{\partial z^2}\left[\zeta - (\sigma_v S)^{-1}\frac{\partial \rho}{\partial z}\right] + \frac{E_H}{2}\left(\frac{\partial^2}{\partial x^2}+\frac{\partial^2}{\partial y^2}\right)\left[\zeta - (\sigma_H S)^{-1}\frac{\partial \rho}{\partial z}\right], \tag{2.6}$$

where

$$\zeta = \frac{\partial v}{\partial x} - \frac{\partial u}{\partial y}. \tag{2.7}$$

The divergence of the horizontal momentum equation similarly yields

$$\zeta = \left(\frac{\partial^2}{\partial x^2}+\frac{\partial^2}{\partial y^2}\right)p - S^{-1}\left[\frac{E_v}{2\sigma_v}\frac{\partial^2}{\partial z^2} + \frac{E_H}{2\sigma_H}\left(\frac{\partial^2}{\partial x^2}+\frac{\partial^2}{\partial y^2}\right) - T\frac{\partial}{\partial t}\right] \times \left[\frac{E_v}{2}\frac{\partial^2}{\partial z^2} + \frac{E_H}{2}\left(\frac{\partial^2}{\partial x^2}+\frac{\partial^2}{\partial y^2}\right) - T\frac{\partial}{\partial t}\right]\frac{\partial \rho}{\partial z}. \tag{2.8}$$

With the hydrostatic relation and (2.8), Eq. (2.6) yields the "master" single governing equation entirely in terms of the pressure. This is most helpful in determining the proper dynamical balances for various time scales and in the several boundary layer regions.

3. The upper Ekman layer

Within a distance of order $E_v^{\frac{1}{2}}$ of $z=1$ the horizontal frictional force due to the vertical mixing of momentum becomes important. For small T the description of this layer is [to $O(T)$], identical to that given in *P*. The salient results required for the present problem are (a) the vertical velocity pumped into the Ekman layer from the interior region below

$$w_I(x,y,1) = \frac{E_v^{\frac{1}{2}}}{2}\mathbf{k}\cdot \mathrm{curl}\,\boldsymbol{\tau}, \tag{3.1}$$

and (b) the horizontal mass flux in the upper Ekman layer

$$\mathbf{M}_E = -\frac{E_v^{\frac{1}{2}}}{2}\mathbf{k}\times\boldsymbol{\tau}. \tag{3.2}$$

4. The lower Ekman layer

A viscous Ekman layer exists on the lower, slanting bottom. Its thickness is $O(E_v^{\frac{1}{2}})$ and for small T the analysis of this layer follows, in all essential respects, the analysis in P. The analysis yields a compatibility condition for the interior velocities on $z=z_s$, namely

$$w_I = u_I\tan\theta + \frac{E_v^{\frac{1}{2}}}{2k\cos\theta}\left[\left(\frac{\partial}{\partial x}+\tan\theta\frac{\partial}{\partial z}\right)\times(v_I + u_I\cos^2\theta + w_I\sin\theta\cos\theta) + \frac{\partial}{\partial y}(v_I - \cos^2\theta u_I - w_I\sin\theta\cos\theta)\right], \quad \text{on} \quad z=z_s, \tag{4.1}$$

where

$$k = [\cos\theta(1+\lambda^{-1}\tan^2\theta)^{\frac{1}{2}}]^{-1}. \tag{4.2}$$

The onshore mass flux in the lower layer, $M_E^{(x)}$, is given by

$$M_E^{(x)} = -\frac{E_v^{\frac{1}{2}}}{2k\cos\theta}(+v_I + u_I\cos^2\theta + w_I\sin\theta\cos\theta)_{z=z_s}. \tag{4.3}$$

5. The interior

In the fluid interior, i.e., the region removed from the upper and lower boundary layers, as well as the side wall boundary layers (the upwelling region), the following balances hold for time scales long compared with one day and short compared with a vertical diffusion time ($1 > T > E_v$):

$$T\frac{\partial u_I}{\partial t} - v_I = -\frac{\partial p_I}{\partial x} \tag{5.1a}$$

$$T\frac{\partial v_I}{\partial t} + u_I = -\frac{\partial p_I}{\partial y} \tag{5.1b}$$

$$\rho_I = -\frac{\partial p_I}{\partial z} \tag{5.1c}$$

$$T\frac{\partial \rho_I}{\partial t} - w_I S = 0 \tag{5.1d}$$

$$\frac{\partial u_I}{\partial x}+\frac{\partial v_I}{\partial y}+\frac{\partial w_I}{\partial z} = 0. \tag{5.1e}$$

Elimination of all variables in favor of p yields

$$\frac{\partial}{\partial t}\left[\left(1+T^2\frac{\partial^2}{\partial t^2}\right)\frac{\partial^2 p_I}{\partial z^2} + S\left(\frac{\partial^2 p_I}{\partial x^2}+\frac{\partial^2 p_I}{\partial y^2}\right)\right] = 0, \tag{5.2}$$

which is the non-dissipative form of (2.6) and (2.8). This is the conservation principle for potential vorticity. For T small with respect to 1, (5.2) may be rewritten as

$$\frac{\partial}{\partial t}\left[\frac{\partial^2 p_I}{\partial z^2}+S\left(\frac{\partial^2 p_I}{\partial x^2}+\frac{\partial^2 p_I}{\partial y^2}\right)\right]=0, \tag{5.3}$$

which serves to filter out only the relatively unimportant internal gravity waves.

On the upper surface, the boundary condition for (5.3) is given by (3.1), which with (5.1c) and (5.1a) becomes

$$w_I=-\frac{T}{S}\frac{\partial^2 p_I}{\partial z\partial t}=E_v^{\frac{1}{2}}W_I(x,y), \quad z=1,\ t>0, \tag{5.4}$$

where $W_I=\mathbf{k}\cdot\text{curl}\boldsymbol{\tau}/2$.

On the lower surface, $z=z_s$, (4.1) implies that for $\tan\theta>E_v^{\frac{1}{2}}$

$$w_I=u_1\tan\theta+O(E_v^{\frac{1}{2}}). \tag{5.5}$$

It is, however, important to determine and include the $O(E_v^{\frac{1}{2}})$ contribution to (5.5) in order to determine the spin-up time of the interior. To do this consistently (5.5) can be substituted into the right-hand side of (4.1) to evaluate w_I therein, to yield w_I to $O(E_v)$, i.e., on $z=z_s$

$$w_I=-\frac{T}{S}\frac{\partial^2 p}{\partial z\partial t}=u_I\tan\theta+\frac{E_v^{\frac{1}{2}}}{2k\cos\theta}\times\left[\left(\frac{\partial}{\partial x}+\tan\theta\frac{\partial}{\partial z}\right)(v_I+u_I)+\frac{\partial}{\partial y}(v_I-u_I)\right]. \tag{5.6}$$

Further, it follows from (5.1a, b) that

$$\left.\begin{aligned} v_I&=\frac{\partial p_I}{\partial x}-T\frac{\partial^2 p_I}{\partial y\partial t}+O(T^2)\\ u_I&=-\frac{\partial p_I}{\partial y}-T\frac{\partial^2 p_I}{\partial x\partial t}+O(T^2)\end{aligned}\right\}, \tag{5.7}$$

which allows (5.6) to be written entirely in terms of the pressure. Conditions (2.5a) and (2.5e) imply that[1] S is small with respect to 1 so that a solution to (5.3) can be found in the form

$$p_I=p_0(x,y)+Sp_1(x,y,z)+\cdots, \tag{5.8}$$

where

$$p_1=Bz-\frac{z^2}{2}\left(\frac{\partial^2}{\partial x^2}+\frac{\partial^2}{\partial y^2}\right)p_0, \tag{5.9}$$

and where B is an arbitrary function of x and y. Application of the boundary conditions (5.4) and (5.6) yields

$$B=\left(\frac{\partial^2}{\partial x^2}+\frac{\partial^2}{\partial y^2}\right)p_0-E_v^{\frac{1}{2}}\frac{t}{T}W_I(x,y), \tag{5.10}$$

$$T\frac{\partial}{\partial t}\left\{\frac{\partial}{\partial x}\left[(1-z_s)\frac{\partial p_0}{\partial x}\right]+(1-z_s)\frac{\partial^2 p_0}{\partial y^2}\right\}-\tan\theta\frac{\partial p_0}{\partial y}+\frac{E_v^{\frac{1}{2}}}{2k\cos\theta}\times\left(\frac{\partial^2 p_0}{\partial x^2}+\frac{\partial^2 p_0}{\partial y^2}\right)=E_v^{\frac{1}{2}}W_I. \tag{5.11}$$

To lowest order the interior is barotropic and the pressure satisfies a topographic, Rossby-wave equation with an Ekman damping term and is forced by the pumping of the upper Ekman layer. Recall that the pumping is switched on at $t=0$ and then held steady.

The solution to (5.11) can be split into a steady part which balances the forcing term, plus an unsteady or time variable part which satisfies the homogeneous initial conditions on the interior currents.

In the interior where x length scales are order 1, the steady part of (5.11), for $\tan\theta\gg E_v^{\frac{1}{2}}$, is (superscript s denotes "steady"),

$$-\frac{\partial p_0^{(s)}}{\partial y}=\frac{E_v^{\frac{1}{2}}}{\tan\theta}W_I(x,y), \tag{5.12}$$

which is identical to the long-term steady solution for the interior, onshore barotropic flow found in P.

The time-variable part of (5.11) is a solution to the homogeneous counterpart of (5.11). For $\tan\theta\ll 1$, this part can be written as

$$p^{(v)}(x,y,t)=\phi(x,y,t)\exp\left(-\frac{E_v^{\frac{1}{2}}}{2k\cos\theta}\frac{t}{T}\right), \tag{5.13}$$

where ϕ satisfies the *inviscid* wave equation

$$T\frac{\partial}{\partial t}\left(\frac{\partial^2\phi}{\partial x^2}+\frac{\partial^2\phi}{\partial y^2}\right)-\tan\theta\frac{\partial\phi}{\partial y}=0. \tag{5.14}$$

The resulting solutions for ϕ, with northward propagating phase, are to be used to cancel at $t=0$, the solution to (5.12). The important point, however, is that this correction field forced by the initial conditions exponentially decays with time so that within a barotropic spin-up time $(2kE_v^{-\frac{1}{2}}\Omega^{-1}\cos\theta)$, the interior (barotropic) solution is given by (5.12). It is this onshore flow, completely specified, which in the steady-state theory of P leads to the poleward countercurrent. The present study shows the not-surprising result that this flow is set up on a much shorter time scale. Since attention will later be focused on the solutions for the quasi-steady period after the spin-up time interval, a

[1] This condition is equivalent to stating that the Rossby radius of deformation $(ND/2\Omega)$ is small compared to L.

further discussion of (5.14) is deleted for the sake of brevity.

With the assumption of interrupted geostrophic contours it follows, as discussed in *P*, that

$$\frac{\partial p_0^{(s)}}{\partial x} \equiv v_0^{(s)} = -\frac{E_v^{\frac{1}{2}}}{\tan\theta}\int_{y_0}^{y}\frac{\partial W_I}{\partial x}(x,y')dy', \quad (5.15)$$

from which it follows, in turn, that the lower Ekman layer is unable to transport an $O(E_v^{\frac{1}{2}})$ mass flux shoreward in the quasi-steady state and hence, will play no significant role in the upwelling mass balance. Since $p^{(v)}$ is $O[p^{(s)}]$, this holds also during the *entire* transient stage.

6. The side wall boundary layers

The interior fields must be supplemented by boundary layer corrections in the vicinity of the side wall layers in order to satisfy the velocity boundary conditions there. For time scales T of order $E_v^{\frac{1}{2}}$ (i.e., on the order of the time required for bottom friction to lead to a quasi-steady state), the single most important region is the hydrostatic boundary layer with a non-dimensional width of order $S^{\frac{1}{2}}$. A thinner diffusion region is required to satisfy the no-slip condition on the longshore velocity, but is dynamically unimportant. All the major mass flux, in both the vertical and horizontal planes, occurs either in this hydrostatic layer region or in the wider topographic layer with a non-dimensional width $E_v^{\frac{1}{2}}L_y^{\frac{1}{2}}/(\tan\theta)^{\frac{1}{2}}$, as in P; L_y is the non-dimensional north-south scale of the forcing (and hence, the motion). These two layers serve to bring the onshore flow to rest at the coast. The thinner dynamically irrelevant diffusion layer then satisfies the no-slip condition on the longshore flow and will not be discussed further.

a. *The hydrostatic layer*

In a region of $O(S^{\frac{1}{2}})$ to $x=1$, the dynamical variables must be supplemented by *correction* variables scaled as

$$\left.\begin{aligned} v &= \bar{v}(\eta,y,z,t) \\ u_g &= S^{\frac{1}{2}}\bar{u}_g(\eta,y,z,t) \\ u_a &= T\bar{u}_a(\eta,y,z,t) \\ p &= S^{\frac{1}{2}}\bar{p}(\eta,y,z,t) \\ \rho &= S^{\frac{1}{2}}\bar{\rho}(\eta,y,z,t) \\ w &= TS^{-\frac{1}{2}}\bar{w}(\eta,z,y,t) \end{aligned}\right\}, \quad (6.1)$$

where

$$\eta = (1-x)S^{-\frac{1}{2}}, \quad (6.2)$$

and where T is $O(E_v^{\frac{1}{2}})$; u_a is the hydrostatic layer's ageostrophic correction to the onshore flow, while u_g is its corresponding geostrophic correction.

These boundary layer variables satisfy

$$\bar{v} = -\frac{\partial\bar{p}}{\partial\eta}, \qquad \bar{u}_g = -\frac{\partial\bar{p}}{\partial y}, \quad (6.3a,b)$$

$$\frac{\partial\bar{v}}{\partial t} = -\bar{u}_a + O(E_v^{\frac{1}{2}}/\lambda\sigma_H S), \qquad \bar{\rho} = -\frac{\partial\bar{p}}{\partial z}, \quad (6.3c,d)$$

$$\frac{\partial\bar{\rho}}{\partial t} = \bar{w} + O(E_v^{\frac{1}{2}}/\lambda\sigma_H S), \qquad \frac{\partial\bar{u}_a}{\partial\eta} = \frac{\partial\bar{w}}{\partial z}, \quad (6.3e,f)$$

from which it follows that

$$\frac{\partial}{\partial t}\left(\frac{\partial^2\bar{p}}{\partial\eta^2} + \frac{\partial^2\bar{p}}{\partial z^2}\right) = 0, \quad (6.4)$$

which could be deduced immediately from (2.7) and (2.8).

The boundary conditions for (6.4) are as follows: At $z=1$ the vertical velocity must vanish yielding

$$\frac{\partial^2\bar{p}}{\partial z\partial t} = 0, \quad z=1, \quad (6.5)$$

while the application of (4.1) to the boundary region at $z=z_s$ yields

$$T\frac{\partial^2\bar{p}}{\partial z\partial t} = -\frac{E_v^{\frac{1}{2}}}{2k\cos\theta}\frac{\partial^2\bar{p}}{\partial\eta^2}, \quad (6.6)$$

under the mild condition that

$$S\tan\theta \ll E_v^{\frac{1}{2}}L_y. \quad (6.7)$$

The solution of (6.4) subject to (6.5) and (6.6) as well as the homogeneous initial conditions must await the derivation of proper boundary conditions on $\eta = O(x=1)$. Before these can be derived, the topographic boundary layer must be discussed.

b. *The topographic layer*

In a region of $O[E_v^{\frac{1}{2}}L_y^{\frac{1}{2}}/(\tan\theta)^{\frac{1}{2}}]$ of $x=1$ [which by (6.7) is much larger than the $S^{\frac{1}{2}}$ layer width], the dynamical variables are supplemented by the dynamical correction variables

$$\left.\begin{aligned} v &= \hat{V}\hat{v}(\xi,y,z,t) \\ u_g &= \hat{V}\Delta\hat{u}_g(\xi,y,z,t) \\ u_a &= \hat{V}T\hat{u}_a(\xi,y,z,t) \\ p &= \hat{V}\Delta\hat{p}(\xi,y,z,t) \\ \rho &= \hat{V}\Delta\hat{\rho}(\xi,y,z,t) \\ w &= \hat{V}\frac{T\Delta}{S}\hat{w}(\xi,y,z,t) \end{aligned}\right\}, \quad (6.8)$$

where

$$\left.\begin{aligned}\xi&=(1-x)/\Delta\\ \Delta&=E_v^{\frac{1}{4}}L_y^{\frac{1}{2}}/(\tan\theta)^{\frac{1}{2}}\end{aligned}\right\}. \tag{6.9}$$

These correction functions satisfy

$$\hat{v}=-\frac{\partial\hat{p}}{\partial\xi},\qquad \frac{\partial\hat{v}}{\partial t}=-\hat{u}_a, \tag{6.10a,b}$$

$$\hat{u}_g=-\frac{\partial\hat{p}}{\partial y},\quad \frac{\partial\hat{\rho}}{\partial t}-\hat{w}=0, \tag{6.10c,d}$$

$$\hat{\rho}=-\frac{\partial\hat{p}}{\partial z},\qquad \frac{\partial\hat{u}_a}{\partial\xi}=\frac{\Delta^2}{S}\frac{\partial\hat{w}}{\partial z}, \tag{6.10e,f}$$

from which it follows that

$$\frac{\partial}{\partial t}\left(\frac{\partial^2\hat{p}}{\partial\xi^2}+\frac{\Delta^2}{S}\frac{\partial^2\hat{p}}{\partial z^2}\right)=0. \tag{6.11}$$

Since by (6.7) $\Delta^2\gg S$, (6.11) implies that the topographic layer, like the interior, is barotropic to lowest order, and in fact, the equation for this barotropic layer can easily be shown to be the boundary layer scaled version of (5.11), namely

$$\left(\frac{T}{E_v^{\frac{1}{2}}}\right)d_0\frac{\partial}{\partial t}\frac{\partial^2\hat{p}}{\partial\xi^2}-L_y\frac{\partial\hat{p}}{\partial y}+\frac{1}{2k\cos\theta}\frac{\partial^2\hat{p}}{\partial\xi^2}=0, \tag{6.12}$$

where $d_0=(1-\tan\theta)$. Recall that T is $O(E_v^{\frac{1}{2}})$ and L_y is the nondimensional y scale. Just as the interior, the topographic layer solution can be partitioned into a steady part $\hat{p}^{(s)}$, and a time-dependent part $\hat{p}^{(v)}$. The steady part satisfies

$$\frac{\partial^2 p^{(s)}}{\partial\xi^2}-L_y(2k\cos\theta)\frac{\partial\hat{p}^{(s)}}{\partial y}=0, \tag{6.13}$$

which aside from minor notational differences, is the same boundary layer equation given in P for the long-term steady-state solution. The function $\hat{p}^{(s)}$ serves, in the quasi-steady state, to help satisfy the condition of no normal flow at the coast for the barotropic component of the flow. The time-variable function $\hat{p}^{(v)}$ serves only to cancel $\hat{p}^{(s)}$ at $t=0$. As the interior time-variable barotropic flow, it will decay away in a barotropic spin-up time.

It was shown in P that the solution to (6.13) for $\hat{p}^{(s)}$ leads to a representation for $\hat{v}^{(s)}$ in the form

$$\hat{v}^{(s)}=-\left(\frac{2}{\pi}\right)^{\frac{1}{2}}(L_y 2k\cos\theta)^{\frac{1}{2}}\int_{y_0}^{y}\frac{\hat{u}_g^{(s)}(0,y')}{(y-y')^{\frac{1}{2}}}\times\exp\left[-\frac{\xi^2 L_y 2k\cos\theta}{(y-y')}\right]dy', \tag{6.14}$$

so that the essential question in determining the direction of the barotropic flow in the topographic layer is the sign of the topographic layer's correction to the onshore flow at the coast (i.e., at $x=1$ or $\xi=0$). Both the determination of this function and the proper boundary conditions for the hydrostatic layer require consideration now of the matching condition on the onshore velocity at the coast.

7. The matching condition

The matching condition of interest is the condition of no normal flow at the coast. At the coast, $x=1$, the onshore flow consists of the flow from the interior (barotropic), along with contributions from the hydrostatic and topographic layers. As was shown in P the sum of these contributions at $x=1$ must match to a corner sink of fluid which represents, at $x=1$, $z=1$, the upwelling fluid sucked into the upper Ekman layer there. That is, at $x=1$,

$$u_I+\hat{V}(T\hat{u}_a+\Delta\hat{u}_g)+(S^{\frac{1}{2}}\bar{u}_g+T\bar{u}_a)=-\frac{E_v^{\frac{1}{2}}}{2}\tau^{(y)}\delta(1-z). \tag{7.1}$$

The term on the right-hand side is the corner sink whose strength is proportional to the offshore Ekman flux at the coast. It follows from (6.3) that

$$\int_{z_s}^{1}\bar{u}_a(0,z)=\int_0^{\infty}\bar{w}(\eta,z_s)d\eta=-\int_{z_s}^{1}\frac{\partial\bar{v}}{\partial t}dz. \tag{7.2}$$

Now

$$\int_0^{\infty}\bar{w}(\eta,z_s)d\eta$$

is the total vertical flux of fluid entering the hydrostatic layer at its base. This mass flux must equal the onshore mass flux in the lower Ekman layer produced in turn by the interior and topographic longshore flows. It is a simple matter to show that the reduction in order of the interior flow to $O(E_v^{\frac{1}{4}}/\tan\theta)$ by the topographic vorticity constraint eliminates the bottom Ekman layer as a mass transporter and hence, to the lowest order, (7.2) reduces to

$$\int_{z_s}^{1}\frac{\partial\bar{v}(0,z')}{\partial t}dz'=0. \tag{7.3}$$

This places an interesting constraint on the baroclinic flow in the hydrostatic layer, namely, that at the coast there is no change with time of the barotropic component of the hydrostatic layer. Since the longshore flow is initially zero, the barotropic component of the flow in the hydrostatic layer must *remain* zero at the coast. Of course, there may well be a change in the structure of $\bar{v}$ as η increases seaward, but (7.3)

guarantees that there must be a reversal of longshore flow in the hydrostatic layer with depth at positions near the coast. It is important to note that this holds for times short compared to a diffusion time. Indeed, in the steady state, the calculations in P showed that the longshore baroclinic flow was of a single sign. In the present case the z-average of the boundary layer longshore flow is entirely contained in the topographic layer.

Integrating (7.1) over the interval $(z_s,1)$ at $x=1$ yields [after use of (7.3) and (6.3a, b, c)]

$$-S^{\frac{1}{2}}\int_{z_s}^{1}\frac{\partial\bar{p}}{\partial y}dz+d_0[u_I+\hat{V}(T\hat{u}_a+\Delta\hat{u}_g)]=-\frac{E_v^{\frac{1}{2}}}{2}\tau^{(y)}(1,y). \quad (7.4)$$

Now the ratio of the first term on the left-hand side of (7.4) to the source term on the right-hand side of (7.4) is no larger than

$$\frac{S^{\frac{1}{2}}}{L_yE_v^{\frac{1}{2}}}=\frac{ND}{2\Omega L_{*y}}\left(\frac{D}{\delta_E}\right), \quad (7.5)$$

where L_{*y} is the dimensional north-south scale of the motion, while δ_E is the thickness of the *surface* Ekman layer. For $2\Omega=10^{-4}$ sec^{-1}, $N=10^{-2}$ sec^{-1}, $D=10^4$ cm and $D/\delta_E=10$, this ratio is $O(10^{-1})$ if L_{*y} is of the order of 1000 km. Actually, the first term in (7.4) could be smaller if $\bar{p}$ changes sign in the depth interval causing some cancellation within the interval of integration. The longer y scales are the most effective scales in producing longshore scales (P) and so I restrict further attention to scales at least large enough so that the parameter in (7.5) is small (i.e., scales large compared with 100 km in the north-south direction).

This leads to a simple relation for the steady component of the onshore flow in the topographic layer, i.e.,

$$d_0\hat{u}_g^{(s)}(0,y)=-\frac{E_v^{\frac{1}{2}}}{2}\tau^{(y)}(1,y)$$
$$-d_0u_I^{(s)}(1,y)=-d_0\frac{\partial\hat{p}^{(s)}}{\partial y}(1,y), \quad (7.6)$$

where I have chosen

$$\hat{V}=\Delta^{-1} \quad (7.7)$$

as a convenient scale for the topographic velocities. This, with (6.14) and (5.12), completely determines the longshore pressure gradient as well as the barotropic longshore flow in the topographic layer for time scales long compared with the spin-up time. This barotropic flow is the same as found on the longer time scale[2] in P, i.e., the flow in the topographic layer will be poleward if there is a net *onshore* flow exterior to the upwelling region.

The matching condition (7.1) can therefore be written

$$\left(T\frac{\partial^2\bar{p}}{\partial t}-S^{\frac{1}{2}}\frac{\partial\bar{p}}{\partial y}\right)=-\frac{E_v^{\frac{1}{2}}}{2}\tau^{(y)}(1,y)\delta(1-z)$$
$$-\left(\frac{T}{\Delta}\hat{u}_a+\hat{u}_g\right)-u_I, \quad (7.8)$$

where, recall $T=O(E_v^{\frac{1}{2}})$. The homogeneous solutions of (7.4) yield an internal Kelvin wave structure for $\bar{p}$ (Gill and Clarke, 1973). However, in the present case the time scale is determined [T is $O(E_v^{\frac{1}{2}})$] and the y scale is determined by the forcing.

Thus, when

$$S^{\frac{1}{2}}/(L_yE_v^{\frac{1}{2}})\ll 1, \quad (7.9)$$

which is the case of present interest as a consequence of the discussion following (7.5), it follows that the second term on the left-hand side of (7.8) can be neglected. This is equivalent to the statement that the speed of propagation of internal Kelvin waves for *large* north-south length scales is so slow that the wave nature of the motion is not apparent on time scales as short as the barotropic spin-up time. That is, in a spin-up time, the advance of the phase of the Kelvin wave is a small fraction of the north-south scale L_{*y}.

Since the first term in (7.8) has zero depth average by (7.3), it follows that the right-hand side of (7.8) must have zero depth average also. This implies that the time variable part of the interior onshore flow must cancel the time variable part of the topographic onshore flow at the coast, so that using (7.6), Eq. (7.8) becomes

$$\frac{\partial^2\bar{p}}{\partial\eta\partial t}=-\frac{E_v^{\frac{1}{2}}}{2T}\tau^{(y)}(1,y)[\delta(1-z)-d_0^{-1}], \quad \eta=0, \quad (7.10)$$

which is the required boundary condition for (6.4), (6.5) and (6.6).

8. The hydrostatic layer current

The solution to (6.4), subject to (6.5), (6.6) and (7.10), can be found for arbitrary t in terms of a Fourier sine transform. Sparing the reader the details of the calculation, I find that to $O(S^{\frac{1}{2}}\tan\theta)$ (where for simplicity T has been set *equal* to $E_v^{\frac{1}{2}}$),

$$\bar{p}(\eta,y,z,t)=\tau^{(y)}(1,y)\frac{2}{\pi}\int_0^\infty P(\alpha,z)\cos\alpha\eta d\alpha, \quad (8.1a)$$

[2] In P the application of a surface heating contributed to the forcing of the interior onshore flow. In the present case, i.e., for times small compared with a vertical diffusion time, surface heating plays no role since the thermal structure of the interior is as yet unaffected by the heating.

where

$$P(\alpha,z)=\frac{\sin k\alpha(z-z_s)}{\alpha\cosh\alpha d_0}\left(1-\frac{\sin k\alpha d_0}{\alpha d_0}\right)\left\{\frac{t}{2}-\frac{k\cos\theta}{\alpha\coth\alpha d_0}\times\left[1-\exp\left(-\frac{t\alpha\coth\alpha d_0}{2k\cos\theta}\right)\right]\right\}+\frac{k\cos\theta}{\alpha^2\cosh\alpha d_0}\times\left(1-\frac{\sin k\alpha d_0}{\alpha d_0}\right)\left[1-\exp-\left(\frac{\alpha t\coth\alpha d_0}{2k\cos\theta}\right)\right]\cosh\alpha(z-z_s)+\frac{t}{2d_0}\frac{1}{\alpha^2}[\cosh\alpha(z-z_s)-1]. \quad (8.1b)$$

Note that for small t

$$\bar{p}\sim\tau^{(y)}(1,y)t\frac{2}{\pi}\int_0^\infty d\alpha\left(1-\frac{\sin k\alpha d_0}{\alpha d_0}\right)\frac{\cosh\alpha(z-z_s)}{\alpha\sin k\alpha d_0}\cos\alpha\eta+\frac{\tau^{(y)}(1,y)}{2d_0}\frac{2}{\pi}\int_0^\infty d\alpha\frac{\cos\alpha\eta}{\alpha^2}[\cosh\alpha(z-z_s)-1], \quad (8.2)$$

which is, to be sure, not terribly illuminating. It is helpful, however, for it shows that $\bar{p}$ is linear in t for small t and satisfies $\partial\bar{p}/\partial z=0$ on $z=z_s$, instead of the more complex (6.6). Similarly for large t (the quasi-steady state)

$$\tilde{p}=\frac{t\tau^{(y)}(1,y)}{2}\frac{2}{\pi}\int_0^\infty d\alpha\left(1-\frac{\sin k\alpha d_0}{\alpha d_0}\right)\frac{\cos\alpha\eta}{\cosh\alpha d_0}\sin k\alpha(z-z_s)+\frac{t}{2}\tau^{(y)}(1,y)\frac{2}{\pi}\int_0^\infty d\alpha[\cosh\alpha(z-z_s)-1]\frac{\cosh\alpha\eta}{\alpha^2}, \quad (8.3)$$

so that for large t, $\tilde{p}$ is still growing linearly with time[3] but the effect of bottom friction has been to eliminate the hydrostatic layer's pressure contribution and hence velocity on the bottom, i.e., now $\tilde{p}=0$ on $z=z_s$. This information can be used to achieve a more helpful representation of the quasi-steady solution for the hydrostatic layer (i.e., for large t) for which the boundary condition

$$\tilde{p}=0, \quad z=z_s,$$

may be used instead of (6.6), for then it follows that

$$\bar{p}=\sum_{n=0}^{\infty}A_n e^{-\mu_n\eta}\sin\mu_n(z-z_s), \quad (8.4)$$

where

$$\mu_n=(n+\tfrac{1}{2})\pi/d_0. \quad (8.5)$$

In order to satisfy (7.10)

$$A_n=\frac{t\tau^{(y)}(1,y)}{\mu_n d_0}\left[(-1)^n-\frac{1}{\mu_n d_0}\right], \quad (8.6)$$

so that

$$\bar{v}=-\frac{\partial\bar{p}}{\partial\eta}=\frac{t\tau^{(y)}(1,y)}{d_0}\sum_{n=0}^{\infty}\left[(-1)^n-\frac{1}{d_0\mu_n}\right]\times e^{-\mu_n\eta}\sin\mu_n(z-z_s). \quad (8.7)$$

The infinite series in (8.7) can be summed relatively easily to yield

$$\bar{v}=t\frac{\tau^{(y)}(1,y)}{d_0}\left\{\frac{\sin(\pi Z/2)\sinh(\pi X/2)}{\cos(\pi Z)+\cosh(\pi X)}-\frac{1}{\pi}\tan^{-1}\left[\frac{\sin(\pi Z/2)}{\sinh(\pi X/2)}\right]\right\}, \quad (8.8)$$

where

$$\left.\begin{aligned}Z&=(z-z_s)/d_0\\X&=\eta/d_0\end{aligned}\right\}, \quad (8.9)$$

so that X is the offshore distance in units of the Rossby radius of deformation based on the fluid depth at the coast (d_0D), while Z is the vertical distance from the bottom in units of the coastal depth.

Note that for large X, from (8.8),

$$\bar{v}\sim t\frac{\tau^{(y)}(1,y)}{d_0}\{e^{-\pi X/2}\sin(\pi Z/2)[1-2/\pi]\} \quad (8.10)$$

[which is equivalent to taking only the first term in the sum (8.4)]. For large X, i.e., sufficiently for offshore, the longshore flow contributed by the hydrostatic layer flow is, *at all levels, in the direction of the applied stress*, which is equatorward in the normal situation. Thus for large X, the existence of a countercurrent, after only the barotropic spin-up time, depends on the steady-state contribution of the topographic layer as in P. On the other hand, for small X,

$$\bar{v}\sim\frac{t\tau^{(y)}(1,y)}{d_0}\left\{-\tfrac{1}{2}+X\left[\frac{\pi\sin(\pi Z/2)}{1+\cos(\pi Z)}+\frac{1}{2\sin(\pi Z/2)}\right]\right\}, \quad (8.11)$$

for Z different from zero (where $\bar{v}$ vanishes) and $Z=1$ where $\bar{v}$ has a singular structure at $X=0$, $Z=1$, reflecting the upwelling sink. From (8.11) it follows that for small enough X, below the surface, upwelling singularity, the flow is in the direction *opposite* to the applied wind stress. For small X and z *near* 1 (i.e., near the upwelling sink) (8.8) yields

$$\bar{v}\sim\frac{t\tau^{(y)}(1,y)}{d_0}\left\{\frac{1}{\pi}\frac{X}{[X^2+(1-z)^2]}-\frac{1}{2}\right\}. \quad (8.12)$$

[3] However, $\bar{u}_a$ and $\bar{w}$ are steady.

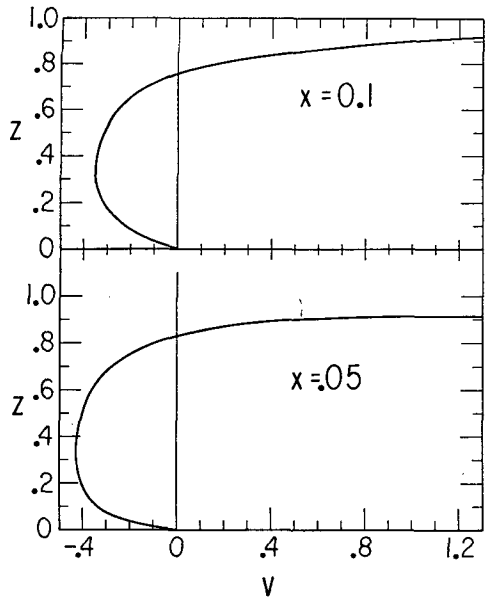

FIG. 2. The hydrostatic layer's longshore velocity profile at $X=0.1$ and 0.05, where X is measured in units of the coastal Rossby deformation, $Nd_0D/(2\Omega)$, and Z is measured in units of coastal depth, d_0D. Positive $\bar{v}$ is flow in the direction of the wind.

For small X and small $(1-z)$ there is an intense surface current flowing in the direction of the applied stress.

Fig. 2 shows the velocity[4] of the hydrostatic layer flow alone at $X=0.1$ and $X=0.05$, i.e., very near the coast, clearly showing the countercurrent. (The contribution of the relatively weaker and broader topographic layer will shift the zero point of v somewhat.) Positive values of $\bar{v}$ imply flow *in the direction* of the wind stress. Fig. 3 shows the velocity profile about one-half a deformation radius offshore. Note that the countercurrent is much weaker. At $X=0.6$ and 0.7 (Fig. 4), the countercurrent appears absent in the graph of v. Analysis of (8.11) shows that the most seaward extent of the countercurrent in the hydrostatic layer occurs at $Z=0$, $X=0.68$. At $X=1$ and 1.5 (Fig. 5),

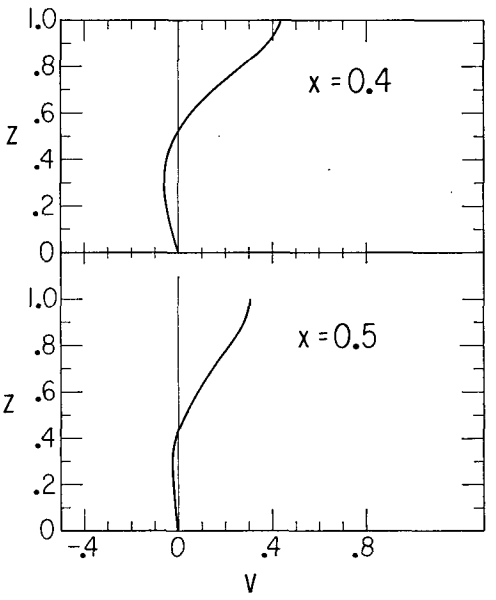

FIG. 3. As in Fig. 2 for $X=0.4$ and 0.5.

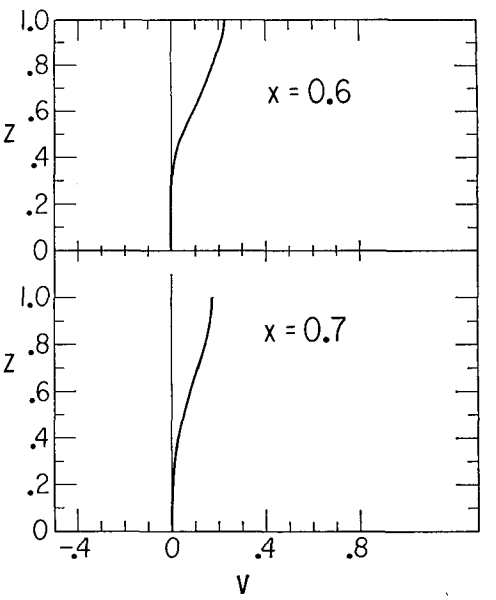

FIG. 4. As in Fig. 2 for $X=0.6$ and 0.7.

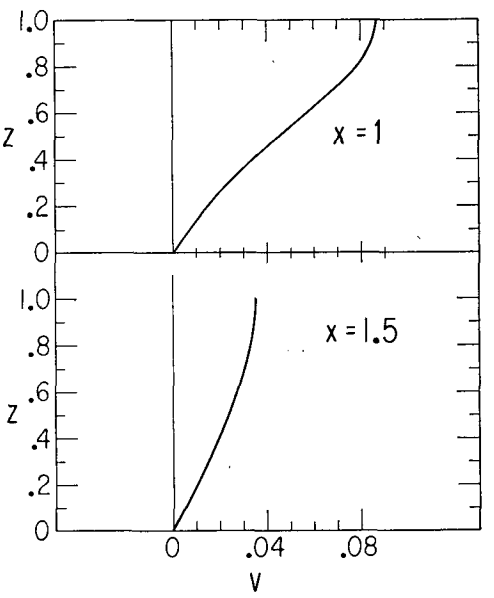

FIG. 5. As in Fig. 2 for $X=1$ and 1.5. Note the expansion in the scale for v.

[4] Actually, these figures are graphs of $d_0\bar{v}/[t\tau^{(y)}(1,y)]$.

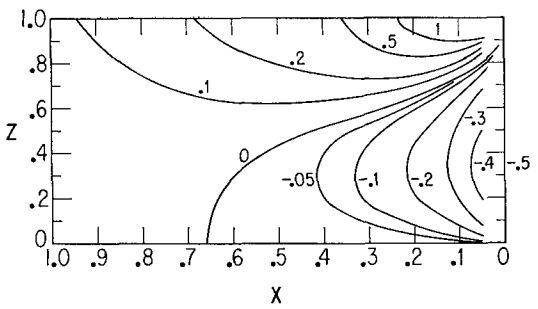

FIG. 6. A cross section showing isopleths of the longshore velocity in the hydrostatic layer.

the flow is of a single sign and in the direction of the wind stress. Indeed, the profile in Fig. 5b is indistinguishable from the asymptotic form given by (8.10), i.e., proportional to $\sin(\pi Z/2)$.

A cross section of the longshore current structure is given in Fig. 6 showing the isolines of constant $\bar{v}$, as given by (8.8).

The important result obtained here is that the action of the topographic constraint on the hydrostatic layer produces, on time scales *long compared to a barotropic spin-up time* but *short compared to a vertical diffusion* time,[5] a countercurrent in the hydrostatic layer which is tucked against the coast. This is in contrast to the solution for the hydrostatic layer which holds for times *small* compared with a spin-up time. An analysis, similar to that leading to (8.8) for large t, shows that for small t before bottom friction acts significantly,

$$\bar{v}=\frac{t\tau^{(y)}(1,y)}{d_0}\left[\frac{e^{\pi X}+\cos\pi Z}{2(\cosh\pi X+\cos\pi Z)}-1\right]. \quad (8.13)$$

For large X, this yields

$$\bar{v}\sim\frac{2t\tau^{(y)}(1,y)}{d_0}e^{-\pi X}\cos\pi Z, \quad (8.14)$$

and there is a countercurrent in $\bar{v}$ even for large X with the flow reversal occuring at mid-depth. As time goes on and bottom friction acts, the flow structure in the hydrostatic layer will change from (8.13) to (8.8), with the hydrostatic layer's countercurrent reaching a quasi-steady state flowing in a region tucked against the coast and disappearing about two-thirds a deformation radius offshore. This contribution to the countercurrent will fade away on the much longer diffusion time scale to achieve the profile given in P.

[5] In principal, the analysis given here for the hydrostatic layer is valid (Allen, 1973b) for times short compared with the lateral diffusion time, based on the width of the hydrostatic layer. In non-dimensional units this yields a time of $O(\lambda SE_v^{-1})$ instead of E_v^{-1}. Although there is an important conceptual distinction between these two time scales, λS is, in most realistic estimates (see Allen 1973b), sufficiently close to 1 that, henceforth, I make no distinction in discussing the interval of validity of the solution (8.8).

Once the longshore current in the hydrostatic layer is determined the vertical upwelling velocity can be determined from (6.3a, c, e). In the case of most interest, i.e., for large t, it follows that

$$\bar{w}=-\frac{\tau^{(y)}(1,y)}{d_0}\left\{\frac{\cos(\pi Z/2)\cosh(\pi X/2)}{\cosh(\pi X)+\cos(\pi Z)}-\frac{1}{\pi}\log\left[\frac{\cosh(\pi X/2)+\cos(\pi Z/2)}{\cosh(\pi X/2)-\cos(\pi Z/2)}\right]\right\}, \quad (8.15)$$

while

$$\bar{u}_a=-\frac{\tau^{(y)}(1,y)}{d_0}\left\{\frac{\sin(\pi Z/2)\sinh(\pi X/2)}{\cosh(\pi X)+\cos(\pi Z)}-\frac{1}{\pi}\tan^{-1}\left[\frac{\sin(\pi Z/2)}{\sinh(\pi X/2)}\right]\right\}. \quad (8.16)$$

Profiles of the vertical velocity are shown in Fig. 7 for the case of upwelling-favorable wind stress for three levels. Note that near the surface the upwelling velocity is intense but narrow. At mid-depth the upwelling is much weaker but broader. At about $Z=0.2$, for small X, the vertical velocity is *downward* (see Fig. 8) reflecting the depression of the isopycnal surfaces associated with the growing poleward countercurrent. This downward flow enters the lower Ekman layer and recirculates vertically at X positions >0.32 where $\bar{w}>0$ for $Z=0$. This circulation implies an offshore Ekman flux near the coast. This is driven by a relatively weak, steady poleward bottom flow which was ignored when (6.6) was replaced by $\bar{p}=0$ for large t.

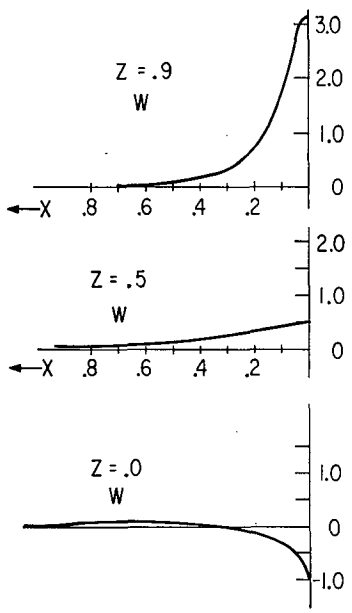

FIG. 7. Profiles of the vertical velocity in the upwelling layer at $Z=0.9$, $Z=0.5$ and $Z=0$.

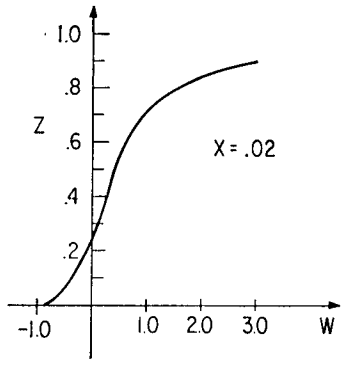

FIG. 8. The vertical velocity as a function of depth at $X=0.02$.

The *total* onshore flow is (in this case of zero wind stress curl) near the coast

$$u=-E_v^{\frac{1}{2}}\frac{\tau^{(y)}(1,y)}{d_0}\left\{\tfrac{1}{2}+\frac{\sin(\pi Z/2)\sinh(\pi X/2)}{\cosh(\pi X)+\cos(\pi Z)}-\frac{1}{\pi}\tan^{-1}\left[\frac{\sin(\pi Z/2)}{\sinh(\pi X/2)}\right]\right\}, \quad (8.17)$$

and is everywhere greater than zero, vanishing on the open interval $0\leqslant Z<1$ for $X=0$. A schematic of the streamline pattern is shown in Fig. 9.

9. Conclusion

This study has examined the evolution of the longshore current produced by upwelling in the presence of bottom topography for times long compared with a barotropic spin-up time $[D/(\nu_v\Omega)^{\frac{1}{2}}]$ but short compared to a vertical diffusion time $[D^2/\nu_v]$. The former time is of the order of a few days, the latter is probably several weeks.

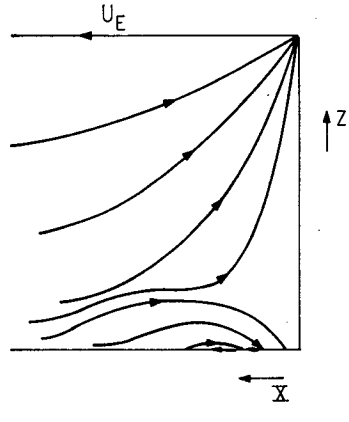

FIG. 9. A schematic of the upwelling circulation for large t.

The analysis shows that in this interval of time the constraint of topography produces a steady, barotropic topographic boundary layer with the same structure as given by the completely steady-state theory. One important difference is that the magnitude of the flow in the topographic layer is not affected at this shorter time by the surface heat flux as it was in the completely steady-state layer found in P. After a vertical diffusion time the north-south surface heating gradients will affect the onshore transports in the interior which, in turn, determine the magnitude and direction of the longshore flow in the topographic layer. It may well be then that the topographic layer will alter its *strength* (and perhaps even direction) in the time interval between the spin-up and diffusion time scales.

The analysis also shows that the hydrostatic layer starts at small t with a *broad* countercurrent, which for t large compared with a spin-up time then shrinks to a quasi-steady structure with the countercurrent restricted to a narrow region near the coast.

Furthermore, for north-south length scales most efficient in driving longshore currents (i.e., *large* longshore scales) the analysis shows the absence of internal Kelvin waves. It may happen, however, that the large-scale forcing will produce smaller scale Kelvin waves due to the scattering transfer of large-scale forcing to a smaller scale longshore response under the influence of longshore irregularities in the topography or coastline.

Acknowledgments. This research was supported in part by the National Science Foundation under Grant GA-28427. I am indebted to John Allen for his suggestion to present explicitly the structure of the upwelling vertical velocity as determined in Section 8.

REFERENCES

Allen, John S., 1973a: Final Report of the Coastal Upwelling Ecosystems Analysis Summer 1973 Theoretical Workshop. School of Oceanography, Oregon State University.

——, 1973b: Upwelling and coastal jets in a continuously stratified ocean. *J. Phys. Oceanogr.*, **3**, 245–257.

Gill, A. E., and A. J. Clarke, 1973: Wind-induced upwelling, coastal currents and sea level changes. Submitted for Publication.

Hurlburt, H. E., and J. D. Thompson, 1973: Coastal upwelling on a β-plane. *J. Phys. Oceanogr.*, **3**, 16–32.

Huyer, A., R. L. Smith, and R. D. Pillsbury, 1973: Observations in a coastal upwelling region during a period of variable winds (Oregon Coast, July 1972). *Tethys* (in press).

Pedlosky, J., 1974: Longshore currents, upwelling and bottom topography. *J. Phys. Oceanogr.*, **4**, 214–226.